

# B-site donor and acceptor doped Aurivillius phase $\text{Bi}_3\text{NbTiO}_9$ ceramics

Haixue Yan<sup>a</sup>, Hongtao Zhang<sup>a</sup>, Zhen Zhang<sup>b</sup>, Rick Ubic<sup>a</sup>, Michael J. Reece<sup>a,\*</sup>

<sup>a</sup> Materials Department, Queen Mary University of London, Mile End Road, London E1 4NS, UK

<sup>b</sup> Shanghai Institute of Ceramics, Chinese Academy of Sciences, 1295 Ding Xi Road, Shanghai 200050, China

Received 12 May 2005; received in revised form 19 July 2005; accepted 24 July 2005

Available online 15 September 2005

## Abstract

The electrical properties of B-site donor and acceptor doped Aurivillius phase  $\text{Bi}_3\text{NbTiO}_9$ -based ceramics have been investigated. The effect of donor and acceptor doping on the dielectric constant, coercive field, dc conductivity and piezoelectric constant are presented. The band gap of  $\text{Bi}_3\text{NbTiO}_9$  (BNTO) is about  $3.4 \pm 0.2$  eV, determined from high-temperature dc conductivity measurements. All of the ceramics are ferroelectrics with high Curie points ( $\sim 900$  °C). In acceptor doped ceramics, a low-temperature peak in the dielectric loss tangent is explained in terms of a Debye-type relaxation that results from an oxygen ion-jump mechanism. The activation energy for the relaxation is calculated as  $0.93 \pm 0.05$  eV. The reduction of the piezoelectric constant below 500 °C is produced by depolarization, which is produced by the switching of thermally unstable non-180° domain walls.

© 2005 Elsevier Ltd. All rights reserved.

**Keywords:** Dielectric properties; Electrical conductivity; Piezoelectric properties; Ferroelectric properties; Aurivillius phase material;  $\text{Bi}_3\text{NbTiO}_9$

## 1. Introduction

The general formula of Aurivillius phase materials is  $(\text{Bi}_2\text{O}_2)^{2+}(\text{A}_{m-1}\text{B}_m\text{O}_{3m+1})^{2-}$ , where A is a mono-, di- or trivalent element (or combination) with cuboctahedral coordination. B is a transition element suited to octahedral coordination, e.g.,  $\text{Fe}^{3+}$ ,  $\text{Cr}^{3+}$ ,  $\text{Ga}^{3+}$ ,  $\text{Ti}^{4+}$ ,  $\text{Nb}^{5+}$ ,  $\text{Ta}^{5+}$ ,  $\text{Mo}^{6+}$ , or  $\text{W}^{6+}$ ; and m is the number of octahedral layers in the perovskite slab. The m value<sup>1</sup> can vary from 1 to 6 and can also be fractional, with compounds with  $m = 1.5$ , 2.5 and 3.5 widely known.<sup>2</sup> Millan et al.<sup>3–5</sup> reported the substitution of  $\text{Bi}^{3+}$  in  $[\text{Bi}_2\text{O}_2]^{2+}$  layers by other cations, such as  $\text{Pb}^{2+}$ ,  $\text{Sb}^{3+}$ ,  $\text{Sn}^{2+}$  or  $\text{Te}^{4+}$ , although Newnham et al.<sup>6</sup> suggested that the bismuth oxide layer is almost inviolate.

Bismuth layer-structured ferroelectrics (BLSF) is the common acronym for the Aurivillius phase materials that are ferroelectric. The spontaneous polarization for BLSFs is along the *a*-axis direction for compounds with an even

number of octahedral layers ( $m = 2n$ , where *n* is an integer) and in the *a*-*c* plane (major component in the [100] direction) for odd layer compounds ( $m = 2n + 1$ ). Compared with the widely used PZT ceramics with perovskite structure, BLSF ceramics are characterized by high Curie points, low dielectric constants, low dielectric losses, low aging, high dielectric breakdown strengths, strong anisotropic electromechanical coupling factors and low temperature coefficients of resonant frequency.<sup>7,8</sup> In recent years, BLSFs have been given much attention because some materials, such as  $\text{SrBi}_2\text{Ta}_2\text{O}_9$  (SBT)<sup>9</sup> and  $\text{La}_{0.75}\text{Bi}_{3.25}\text{Ti}_3\text{O}_{12}$  (BLT),<sup>10</sup> are excellent candidate materials for nonvolatile ferroelectric random access memory (FRAM) applications. BLSFs are also better candidates than PZT ( $\text{Pb}[\text{Zr}, \text{Ti}]\text{O}_3$ ) piezoelectrics for high-temperature piezoelectric applications because of their higher Curie points.

$\text{Bi}_3\text{NbTiO}_9$  was discovered by Aurivillius<sup>11</sup> in 1949. Subbarao and Newnham<sup>12,13</sup> showed it to be a ferroelectric with the highest known Curie point in the BLSF family at that time of 940 °C. However, the information about its electrical properties and the effect of doping is still very limited. In the present study the electrical properties of the  $\text{Bi}_3\text{NbTiO}_9$

\* Corresponding author.

E-mail address: [m.j.reece@qmul.ac.uk](mailto:m.j.reece@qmul.ac.uk) (M.J. Reece).

compound have been studied as a function of donor and acceptor doping on the B-site.

## 2. Experimental procedure

Polycrystalline ceramic samples with nominal formulas  $\text{Bi}_3\text{NbTiO}_9$  (BNT0), donor doped  $\text{Bi}_3\text{Nb}_{1.2}\text{Ti}_{0.8}\text{O}_9$  (BNT0-D) and acceptor doped  $\text{Bi}_3\text{Nb}_{0.8}\text{Ti}_{1.2}\text{O}_9$  (BNT0-A) were prepared by conventional ceramic processing. The starting raw materials were  $\text{Bi}_2\text{O}_3$  of 99.975% purity,  $\text{TiO}_2$  of 99.6% purity and  $\text{Nb}_2\text{O}_5$  of 99.9% purity. The materials were mixed by ball milling in ethanol, dried and sieved to under 250  $\mu\text{m}$ , and then calcined at 900 °C for 4 h. After calcination, the powders were re-milled, dried and sieved to under 500  $\mu\text{m}$ , and then finally pressed into disks of 10 mm diameter in a steel die at a pressure of about 200 MPa. The pressed specimens were sintered at 920–1100 °C for 1 h in air. Electrodes for room-temperature and high-temperature electrical property measurements were fabricated with fired-on silver paste (Johnson Matthey, E1100) and platinum paste (Gwent Electronic Materials Ltd., C2011004D5), respectively.

X-ray diffraction (XRD) patterns for the sintered ceramics were obtained with an X-ray diffractometer (Siemens D5000) using Cu K $\alpha$  radiation. The microstructures of the ceramic specimens were studied using a scanning electron microscope (JEOL JSM 6300). The samples for the SEM study were polished and then thermally etched at about 100 °C below their sintering temperatures for 15 min. Samples for piezoelectric measurements were poled by applying a DC electric field of 8–11 kV/mm for 5–15 min in silicone oil at 200 °C. The piezoelectric constant,  $d_{33}$ , was measured using a piezo  $d_{33}$  meter (ZJ-3B, Institute of Acoustics, Academia Sinica). The DC resistivity,  $\rho$ , was measured as a function of temperature using an electrometer (KEITHLEY, Model 6517A) with contacts to the samples within a high temperature furnace. The dielectric constants, losses and Curie points were measured at different frequencies using an LCR meter (Agilent 4284A). The ferroelectric  $P$ – $E$  hysteresis loops were measured at 200 °C using a ferroelectric hysteresis measurement tester (NPL, UK). Thermal depoling experiments were conducted by holding the poled samples with platinum electrodes for 2 h at various high temperatures, cooling to room temperature, measuring  $d_{33}$ , and repeating the procedure at intervals of 100 °C up to 915 °C for BNT0 and 900 °C for BNT0-D or BNT0-A.

## 3. Results and discussion

Fig. 1 shows the XRD patterns for sintered BNT0, BNT0-D and BNT0-A ceramic powders. In the XRD patterns for BNT0, most of the diffraction peaks match those of the BNT0 structure reported previously<sup>14</sup> with the exception of a small peak (marked as S) at about  $2\theta = 30^\circ$ , which matches the strongest peak (1 1 7) for  $\text{Bi}_4\text{Ti}_3\text{O}_{12}$  (BIT). The doped

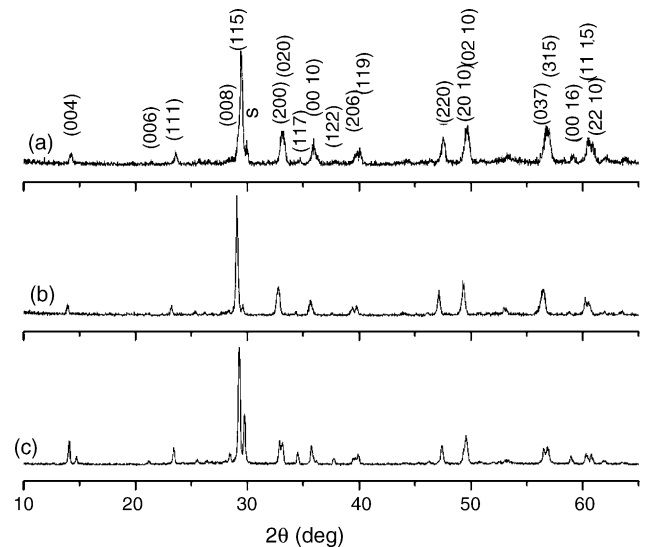


Fig. 1. X-ray powder diffraction patterns of: (a) BNT0, (b) BNT0-D and (c) BNT0-A crushed ceramics sintered at 1100 °C for 1 h.

BNT0-D and BNT0-A ceramics also contain BIT phase. The amount of second phase in BNT0-A is higher than that in BNT0, which may be a consequence of the higher percentage of Ti in BNT0-A compositions. Fig. 2 shows the secondary electron SEM micrographs of BNT0, BNT0-D and BNT0-A ceramics. All the grains are platelike, which is the typical morphology of Aurivillius phase ceramics.

Pure BNT0 has  $A2_1am$  orthorhombic symmetry with the polarization along the  $a$ -axis. Atomic displacements along the  $a$ -axis from the corresponding positions in the parent tetragonal ( $I4/mmm$ ) structure cause ferroelectric spontaneous polarization. Polarization caused by the displacements along the  $b$  and  $c$  axes, in contrast, are cancelled due to the presence of glide and mirror planes, respectively, and thus do not contribute to the total polarization. Based on the atomic displacements, the total polarization of the displacive-type ferroelectric  $\text{Bi}_3\text{NbTiO}_9$  was calculated using Y. Shimakawa's model,<sup>15</sup>

$$P_s = \sum_i \frac{(m_i \times \Delta x_i \times Q_i e)}{V} \quad (1)$$

where  $m_i$  is the site multiplicity,  $\Delta x_i$  is the atomic displacement along the  $a$ -axis from the corresponding position in the tetragonal structure,  $Q_i e$  is the ionic charge of the  $i$ th constituent ion, and  $V$  is the volume of the unit cell. Based on the crystal structure parameters of  $\text{Bi}_3\text{NbTiO}_9$  reported by Wolfe et al.,<sup>12</sup> which are different from Thompson et al.,<sup>16</sup> the atomic displacements along the  $a$ -axis and the contributions of each constituent ion to the total ferroelectric polarization are shown in Fig. 3(a) and (b), respectively. The total spontaneous polarization is estimated as 38.7  $\mu\text{C}/\text{cm}^2$ .

Fig. 4 shows the  $P$ – $E$  hysteresis loops of BNT0, BNT0-D and BNT0-A ceramics at 200 °C. Due to the limited sample thickness we could use (0.10–0.15 mm) because of polishing damage, maximum voltage available (4 kV), conductivity at

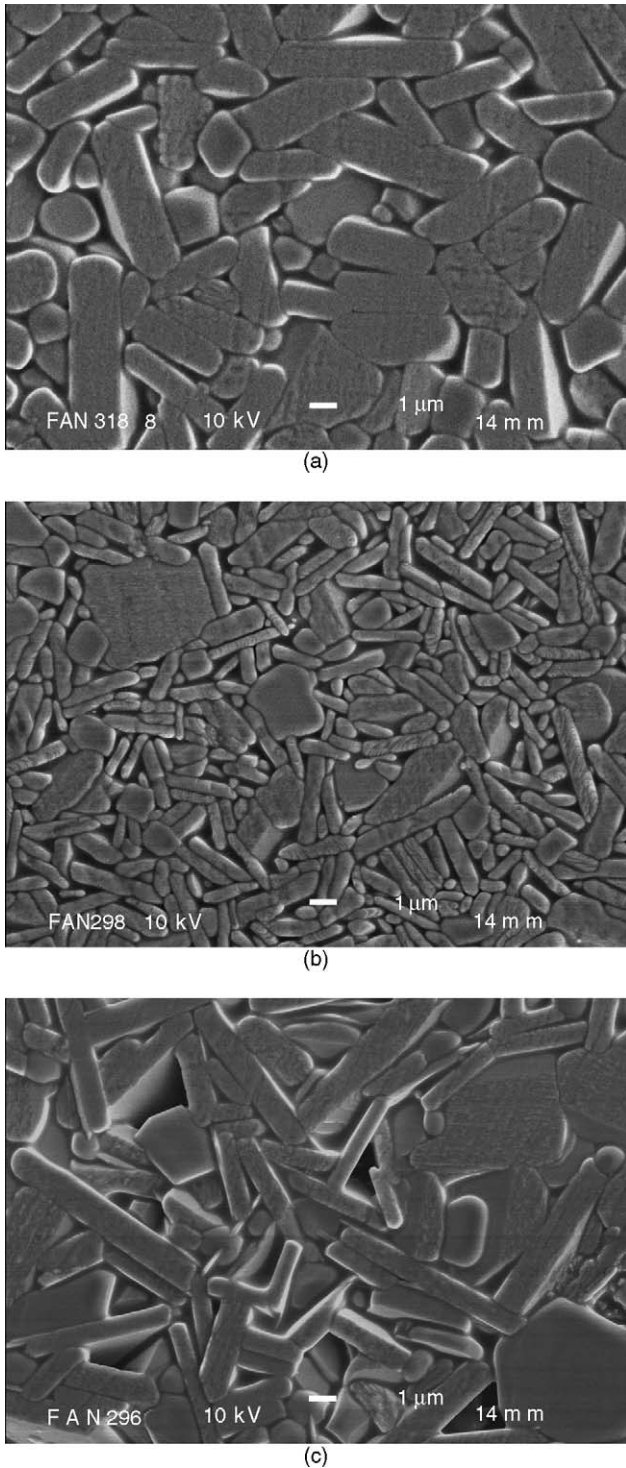


Fig. 2. Secondary electron SEM micrographs showing typical microstructures for: (a) BNT0 (1100 °C), (b) BNT0-D (1100 °C) and (c) BNT0-A (1080 °C) ceramics.

high voltages, and high coercive field ( $E_c$ ), it was not possible to obtain saturated  $P$ – $E$  hysteresis loops. Similar problems have been noted previously for Aurivillius phase materials.<sup>17</sup> The values of  $P_r$  are consequently much less than the theoretical spontaneous polarizations calculated in Fig. 3. It has

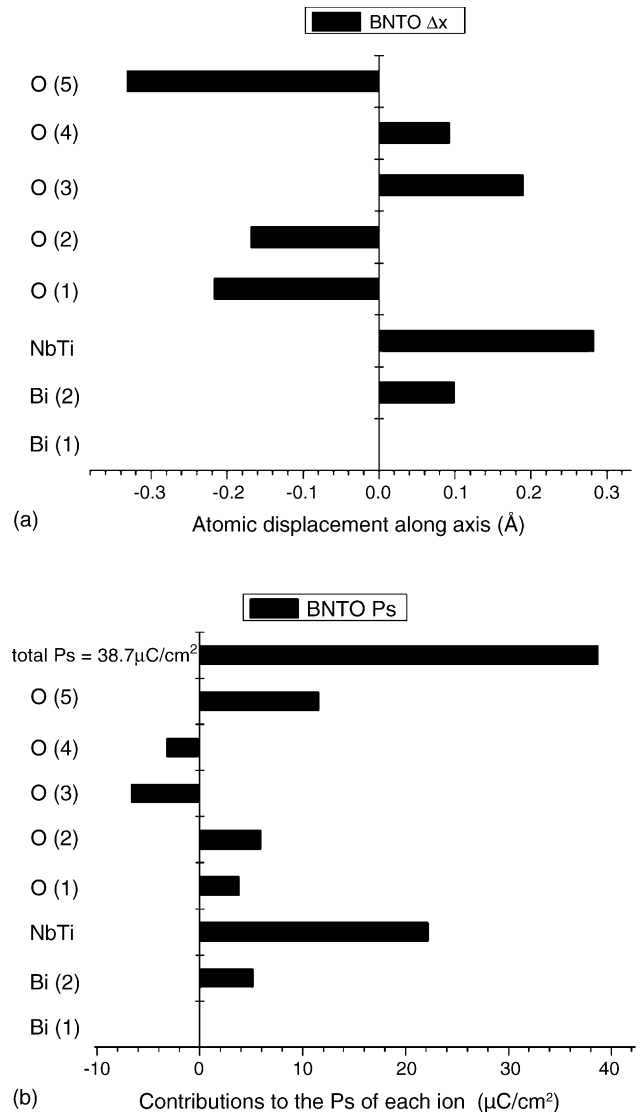


Fig. 3. Schematic drawing of: (a) ion displacement and (b) contribution to the total spontaneous polarization  $P_s$  of each ion of  $\text{Bi}_3\text{NbTiO}_9$ .

been reported that  $\text{Bi}_4\text{Ti}_3\text{O}_{12}$ <sup>18</sup> and  $\text{SrBi}_4\text{Ti}_4\text{O}_{15}$ <sup>19</sup> ceramics exhibit p-type electronic conductivity; therefore, donor doping should decrease conductivity while acceptor doping should increase it. Because of the effect of conductivity in BNT0-A, the apparent polarization increased strongly with decreasing frequency for the  $P$ – $E$  loops. Although none of the  $P$ – $E$  hysteresis loops are fully saturated, the BNT0 and BNT0-D show small peaks in the  $I$ – $E$  loops, which are indicative of some degree of domain switching. No such current peaks were observed for BNT0-A. It can be therefore concluded that the coercive field  $E_c$  of BNT0-A is greater than that of BNT0. This is because of the domain wall pinning caused by the oxygen vacancies ( $V_{\text{O}}^{\bullet\bullet}$ ) in BNT0-A, which makes the movement of domain walls more difficult. However, the  $E_c$  of donor doped BNT0-D is lower than that of BNT0 because the bismuth vacancies ( $V_{\text{Bi}}^{\prime\prime\prime}$ ) make the movement of domain walls easier.

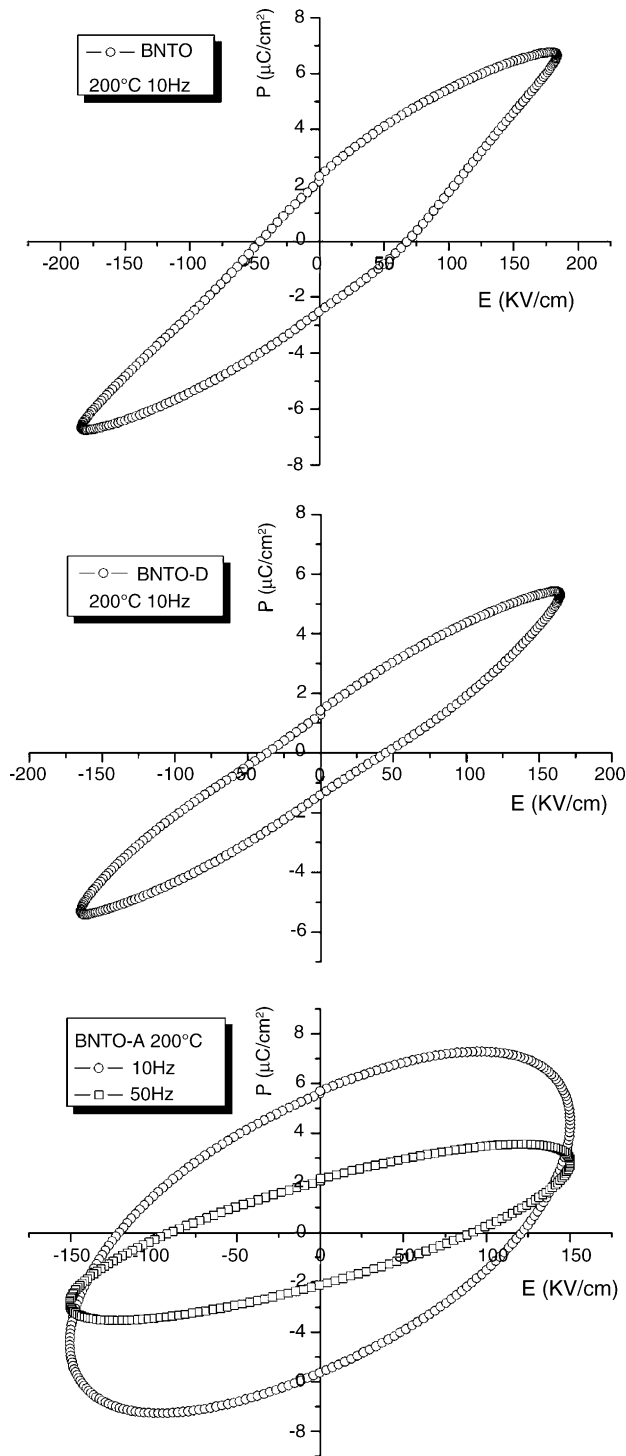


Fig. 4.  $P$ - $E$  hysteresis loops of BNT0, BNT0-D and BNT0-A ceramics.

Fig. 5 shows the temperature dependence of DC resistivity of BNT0, BNT0-D and BNT0-A ceramics. The resistivity of BNT0-A is the lowest among the three materials. This can be attributed to the increase in the concentration of charge carriers. Acceptor doping further increases the concentration of holes in BNT0-A. The resistivity of BNT0-D is greater than that of BNT0 in the low temperature range,

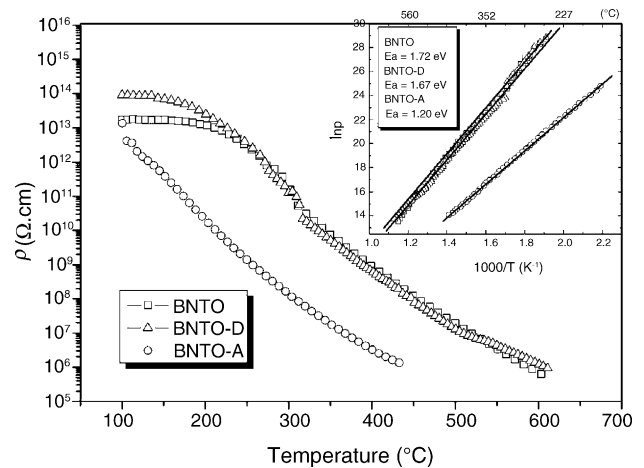


Fig. 5. Temperature dependence of DC resistivity of BNT0, BNT0-D and BNT0-A ceramics.

which is a consequence of the compensating donor doping in BNT0-D. The conductivity activation energy  $E_a$  at high temperature was obtained from an Arrhenius plot (see in Fig. 5). The conductivity activation energy  $E_a$  is  $1.7 \pm 0.1$  eV for the BNT0 and BNT0-D ceramics. The intrinsic electronic conductivity activation energy is equal to half the energy of the band gap,  $E_g$ ; therefore, the band gap of BNT0 and BNT0-D is  $3.4 \pm 0.2$  eV. This value fits in well with those of  $\text{Bi}_4\text{Ti}_3\text{O}_{12}$ ,  $\text{BaBi}_4\text{Ti}_4\text{O}_{15}$  and  $\text{BaTiO}_3$ , which are all about 3.3 eV.<sup>20</sup> The similarity of the band gap is due to the common  $\text{TiO}_6$  octahedra.<sup>20</sup> The activation energy,  $E_a$ , of  $1.2 \pm 0.1$  eV for BNT0-A is close to the high-temperature dc conductivity activation energy (1.0 eV) reported for acceptor doped BIT.<sup>18</sup>

Fig. 6 shows the room-temperature dielectric properties of BNT0, BNT0-D and BNT0-A ceramics sintered at different temperatures. The dielectric constants of BNT0 are lower than those of BNT0-D and higher than those of BNT0-A. The reason for the differences in the dielectric properties is that the bismuth vacancies ( $V_{\text{Bi}}'''$ ) produced by donor doping make domain wall movement easier, but the oxygen vacancies ( $V_{\text{O}}^{\bullet\bullet}$ ) produced by acceptor doping make the domain wall movement more difficult.<sup>21</sup> An oxygen vacancy-acceptor ion dipole may interact with polarization within a domain and make movement of the domain wall more difficult. The frequency dependence of dielectric constants of BNT0-A is also weaker than that of BNT0-D because of domain wall pinning. The weak frequency dependence of dielectric constant of BNT0-A also shows that the dielectric constant was dominated by the main phase rather than the second phase, Nb doped BIT, which is relatively ferroelectrically soft and strongly frequency dependent.

With increasing sintering temperature, the dielectric constants decrease (Fig. 6). The optimum sintering temperatures determined by the highest density are about  $1020^\circ\text{C}$  for BNT0 and BNT0-D and  $980^\circ\text{C}$  for BNT0-A. This suggests that it is the effect of grain size rather than ceramic density caused the dielectric constants to decrease with sintering temperatures. Based on the research of the dielectric

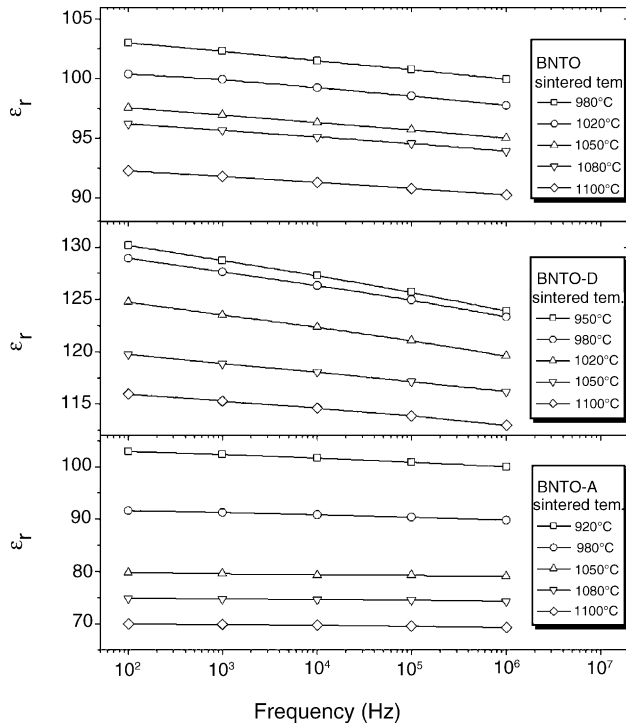


Fig. 6. Room temperature dielectric properties of BNT0, BNT0-D and BNT0-A ceramics.

constants of ferroelectric BaTiO<sub>3</sub> and PbTiO<sub>3</sub> ceramics, the dielectric constants have a maximum value at a critical grain size.<sup>22,23</sup> When the grain size is smaller than this critical size ferroelectric domains are absent. The dielectric constants then increase with increasing grain size because of increasing internal stress.<sup>24</sup> However, when the grain size is larger than the critical value ferroelectric domains are nucleated, the internal stresses decrease and the dielectric constants decrease. Based on the domain wall model,<sup>25</sup> the extrinsic contribution from the 90° domain walls to the dielectric constant is proportional to the total area of 90° walls/volume,  $A_{tot}$ . With increasing sintering temperature, the grain size and the domain size increases. Therefore,  $A_{tot}$  and the contribution from domain walls to the dielectric constant decrease. In Bi<sub>3</sub>NbTiO<sub>9</sub> ceramics, the presence of 90° domain walls was also confirmed based on a transmission electron microscopy (TEM) study.<sup>26</sup> Therefore, the observed decrease in the dielectric constants with increasing sintering temperature of the BNT0 ceramics can be attributed to a decreased contribution from the domain walls with increasing grain size.

Figs. 7–9 show the temperature dependence of dielectric constant and loss of BNT0, BNT0-D and BNT0-A at different frequencies. The peak of the dielectric constant at the Curie point is clear for the higher frequencies, although it is masked by conductivity at the lower frequencies. The Curie points for the BNT0, BNT0-D and BNT0-A ceramics are 913, 886, and 900 °C, respectively. All of the Curie points are frequency independent. Compared with pure BNT0 ceramic, the  $T_c$  of BNT0-A is lower, although some acceptor-dopants

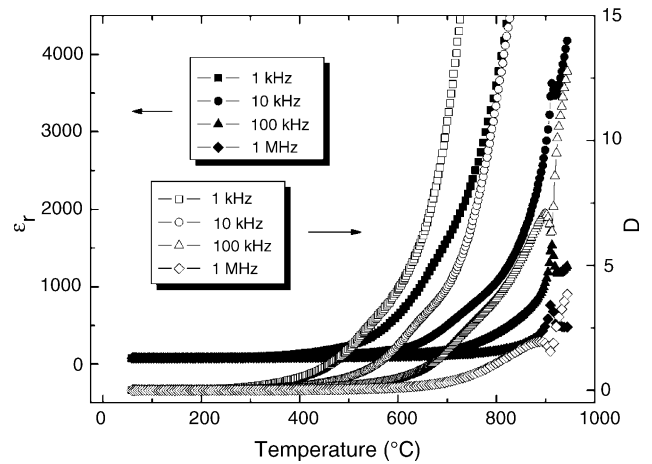


Fig. 7. Temperature dependence of dielectric constant and loss of BNT0 at different frequencies.

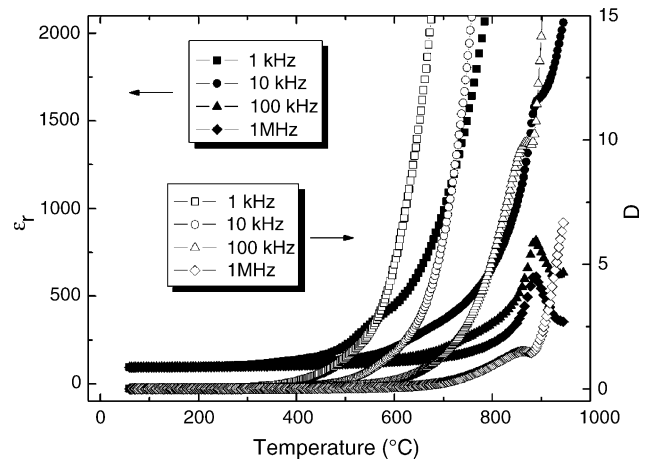


Fig. 8. Temperature dependence of dielectric constant and loss of BNT0-D at different frequencies.

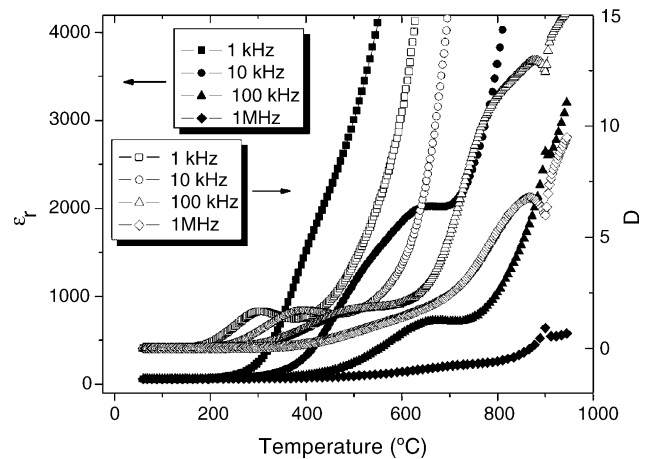


Fig. 9. Temperature dependence of dielectric constant and loss of BNT0-A at different frequencies.

can increase the Curie point of Aurivillius phase materials.<sup>27</sup> This suggests that the amount or nature of dopant might be critical to this behaviour. Above the Curie point the losses increase dramatically because of the contribution from conductivity. There is a loss peak at a few degrees below the Curie point for all compositions. A possible explanation for these peaks is the movement of the ferroelectric domain walls. Displacement of domain walls contributes to the dielectric and mechanical losses of ferroelectric materials and, particularly near the phase transition temperature, may dominate other loss mechanisms.<sup>21</sup> According to Newnham's results,<sup>6</sup> the phase transition at the Curie-point is second-order for the BLSF's compounds with an even number of layers. The  $\text{Bi}_3\text{NbTiO}_9$  is such a compound, so the phase transition at the Curie point for BNTO should be second-order. For the materials with second- or weak first-order ferroelectric phase transitions, there is a dielectric loss peak, as we observe here, at a few degrees below  $T_c$ , which is typically attributed to the movement of domain walls.<sup>28</sup>

For BNTO-A there is a peak in the dielectric constants in the 600–700 °C temperature range (Fig. 9). This is close to the Curie point of pure  $\text{Bi}_4\text{Ti}_3\text{O}_{12}$  (675 °C).<sup>18</sup> It may therefore be a contribution from the B site Nb doped  $\text{Bi}_4\text{Ti}_3\text{O}_{12}$ -based second phase in the BNTO-A ceramics. There is also a set of loss peaks that are clearly distinguished between 200 and 600 °C. According to the results of Shulman et al.,<sup>29</sup> there are no loss peaks within this temperature range for Nb doped BIT, so these loss peaks must originate from the contribution of the main BNTO-A phase. The position of the loss peaks shifts to higher temperatures as the frequency is increased. This is typical of a thermally activated Debye relaxation. When the logarithms of the frequencies are plotted versus the reciprocal of the peak temperature, a straight line is obtained (Fig. 10). The relaxation fits an Arrhenius relationship:

$$w = w_0 \exp\left(\frac{-E_a}{kT}\right) \quad (2)$$

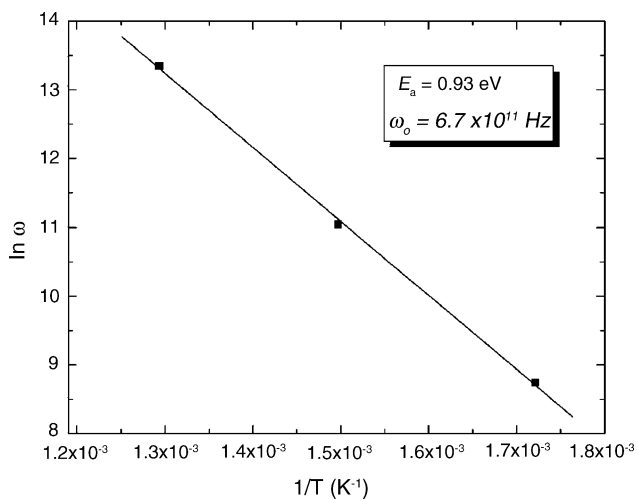


Fig. 10. Logarithm of the peak in frequency vs. reciprocal temperature of the peak (from Fig. 9) showing an Arrhenius relationship.

where  $E_a$  is the activation energy,  $k$  the Boltzmann's constant,  $T$  the absolute temperature at which the relaxation peak has maximum loss, and  $\omega_0$  the angular frequency. The fitted activation energy,  $E_a$ , is  $0.93 \pm 0.05$  eV and the angular frequency,  $\omega_0$ , is  $6.7 \times 10^{11}$  Hz. The frequency range of lattice vibrations for ionic solids is on the order of  $10^{11}$ – $10^{13}$  Hz;<sup>30</sup> therefore the fitted values are in good agreement with parameters that are attributed to an oxygen ion-jump mechanism. In pure  $\text{Bi}_4\text{Ti}_3\text{O}_{12}$  ceramics similar low temperature loss peaks were found and attributed to the ion-jump of oxygen ions ( $\omega_0 = 0.9 \times 10^{11}$  Hz,  $E_a = 0.73$  eV).<sup>29</sup> Research on the internal friction of  $\text{SrBi}_2\text{Ta}_2\text{O}_9$  (SBT)<sup>31,32</sup> showed that the activation energy for the migration of oxygen vacancies is from 0.95 to 0.97 eV, which is very close to our fitted activation energy of  $0.93 \pm 0.05$  eV.

The piezoelectric constant  $d_{33}$  of BNTO, BNTO-D and BNTO-A ceramics are  $5.2 \pm 0.2$ ,  $6.8 \pm 0.2$  and  $1.2 \pm 0.2$  pC/N, respectively. The thermal depoling behaviour of the samples is shown in Fig. 11, in which the piezoelectric constants are plotted against annealing temperature. The BNTO-D is much less stable to thermal depolarisation compared with BNTO and BNTO-A. In ferroelectric materials, domain wall movement can produce a significant contribution to the piezoelectric properties.<sup>33,34</sup> In Aurivillius phase materials, even-layer materials, such as  $\text{SrBi}_4\text{Ti}_4\text{O}_{15}$  ( $m = 4$ ), show relatively little piezoelectric hysteresis.<sup>35,36</sup> A possible reason for this linear stable behaviour is the absence of a contribution from the piezoelectrically active non-180° domain walls. This is not the case for the odd-layer materials, such as  $\text{Bi}_4\text{Ti}_3\text{O}_{12}$  ( $m = 3$ ), which has several types of non-180° domain walls.<sup>36,37</sup> The frequency dependence of the dielectric constant of BNTO-D (Fig. 6) suggest that there is a significant contribution from non-180° domain walls to the properties at room temperature. We suggest that these domain walls are thermally unstable well below the Curie point, and give rise to the observed degradation of  $d_{33}$  below 400 °C. For the BNTO there is a smaller corresponding decrease of  $d_{33}$

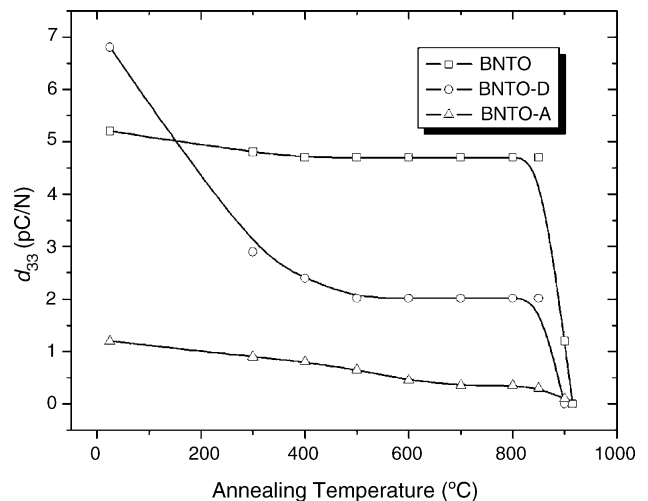


Fig. 11. Effect of annealing temperature (for 2 h) on the  $d_{33}$  of BNTO system ceramics.

with temperature up to 400 °C. This suggests a smaller contribution from the piezoelectrically active non-180° domain walls, which is consistent with the relatively smaller frequency dependence of the permittivity (Fig. 6). The  $d_{33}$  value of BNT0-A decreases continuously up to the Curie point. There is a slight drop in the  $d_{33}$  at about 600 °C, which may be attributed to the depoling of the Nb doped BIT second phase as the temperature approaches its Curie point.<sup>38</sup>

#### 4. Conclusion

Donor and acceptor doping of Bi<sub>3</sub>NbTiO<sub>9</sub> was found to have a significant influence on their properties. The dielectric constants were increased and coercive fields decreased due to the effect of bismuth vacancies produced by donor doping with Nb on the B-site. However, acceptor doping led to a decrease in the dielectric constant and increase in coercive field because of the effect of oxygen vacancies, which make the movement of domain walls more difficult. With increasing sintering temperature, the dielectric constants decreased due to a decrease in the extrinsic contribution from domain wall movement. The spontaneous polarization of Bi<sub>3</sub>NbTiO<sub>9</sub> was calculated as 38.7 μC/cm<sup>2</sup> using previously reported crystal parameters. Based on the high-temperature dc conductivity, the band gap of BNT0 was determined to be 3.4 ± 0.2 eV. All the ceramics are high  $T_c$  ferroelectrics. A loss peak several degrees below the Curie point is probably due to domain wall movement. In acceptor doped BNT0-A, a loss peak at low temperature could be attributed to the jump of oxygen vacancies. The thermal depoling experiments showed a rapid decrease in the  $d_{33}$  of the BNT0 and BNT0-A materials near the Curie point. The BNT0-D showed a significant decrease of  $d_{33}$  at much lower temperatures (<400 °C) because of the presence of ferroelectric active non-180° domain walls which are thermally unstable.

#### Acknowledgement

This research was funded by the Ministry of Defence and QinetiQ Ltd. under contract number CU004-16541. © 2004 QinetiQ Ltd.

#### References

- Wu, Y., Forbess, M. J., Seraji, S., Limmer, S. J., Chou, T. P., Nguyen, C. et al., Doping effect in layer structured SrBi<sub>2</sub>Nb<sub>2</sub>O<sub>9</sub> ferroelectrics. *J. Appl. Phys.*, 2001, **90**, 5296–5302.
- Kikuchi, T., Watanabe, A. and Uchida, K., A family of mixed-layer type bismuth compounds. *Mater. Res. Bull.*, 1977, **12**, 299–304.
- Duran-Martin, P., Castro, A., Millan, P. and Jimenez, B., Influence of Bi-site substitution on the ferroelectricity of the Aurivillius compound Bi<sub>2</sub>SrNb<sub>2</sub>O<sub>9</sub>. *J. Mater. Res.*, 1998, **13**, 2565–2571.
- Millan, P., Ramirez, A. and Castro, A., Substitution of smaller Sb<sup>3+</sup> and Sn<sup>2+</sup> cations for Bi<sup>3+</sup> in Aurivillius-like phases. *J. Mater. Sci. Lett.*, 1995, **14**, 1657–1660.
- Millan, P. and Castro, A., The first doping of lead<sup>2+</sup> into the bismuth oxide layers of the Aurivillius oxides. *Mater. Res. Bull.*, 1993, **28**, 117–122.
- Newnham, R. E., Wolfe, R. W. and Dorrian, J. F., Structural basis of ferroelectricity in the bismuth titanate family. *Mater. Res. Bull.*, 1971, **6**, 1029–1039.
- Takenaka, T. and Sakata, K., Grain orientation effects on electrical properties of bismuth layer-structured ferroelectric Pb<sub>(1-x)</sub>(NaCe)<sub>x/2</sub>Bi<sub>4</sub>Ti<sub>4</sub>O<sub>15</sub> solid solution. *J. Appl. Phys.*, 1984, **55**, 1092–1099.
- Frit, B. and Mercurio, J. P., The crystal chemistry and dielectric properties of the Aurivillius family of complex bismuth oxides with perovskite-like layered structures. *J. Alloys Compd.*, 1992, **188**, 27–35.
- Dearaujo, C., Cuchiaro, J. D., Mcmillan, L. D., Scott, M. C. and Scott, J. F., Fatigue-free ferroelectric capacitors with platinum electrodes. *Nature*, 1995, **374**, 627–629.
- Park, B. H., Kang, B. S., Bu, S. D., Noh, T. W., Lee, J. and Jo, W., Lanthanum-substituted bismuth titanate for use in non-volatile memories. *Nature*, 1999, **401**, 682–684.
- Aurivillius, B., Mixed bismuth oxides with layer lattices. *Arki Kemi*, 1949, **1**, 463–480.
- Wolfe, R. W., Newnham, R. E. and Smith, D. K., Crystal structure of Bi<sub>3</sub>TiNbO<sub>9</sub>. *Ferroelectrics*, 1971, **3**, 1–7.
- Subbarao, E. C., A family of ferroelectric bismuth compounds. *J. Phys. Chem. Solids*, 1962, **23**, 665–676.
- Zhang, Z., Yan, H., Dong, X. and Wang, Y., Preparation and electrical properties of bismuth layer-structured ceramic Bi<sub>3</sub>NbTiO<sub>9</sub> solid solution. *Mater. Res. Bull.*, 2003, **38**, 241–248.
- Shimakawa, Y., Kubo, Y., Nakagawa, Y., Goto, S., Kamiyama, T., Asano, H. et al., Crystal structure and ferroelectric properties of ABi<sub>2</sub>Ta<sub>2</sub>O<sub>9</sub> (A=Ca, Sr, and Ba). *Phys. Rev. B*, 2000, **61**, 6559–6564.
- Thompson, J. G., Rae, A. D., Withers, R. L. and Craig, D. C., Revised structure of Bi<sub>3</sub>TiNbO<sub>9</sub>. *Acta Cryst. B*, 1991, **47**, 174–180.
- Pardo, L., Castro, A., Millan, P., Alemany, C., Jimenez, R. and Jimenez, B., (Bi<sub>3</sub>TiNbO<sub>9</sub>)<sub>x</sub>(SrBi<sub>2</sub>Nb<sub>2</sub>O<sub>9</sub>)<sub>1-x</sub> Aurivillius type structure piezoelectric ceramics obtained from mechanochemically activated oxides. *Acta Mater.*, 2000, **48**, 2421–2428.
- Shulman, H. S., Testorf, M., Damjanovic, D. and Setter, N., Microstructure electrical conductivity and piezoelectric properties of bismuth titanate. *J. Am. Ceram. Soc.*, 1996, **79**, 3124–3128.
- Voisard, C., Damjanovic, D. and Setter, N., Electrical conductivity of strontium bismuth titanate under controlled oxygen partial pressure. *J. Eur. Ceram. Soc.*, 1999, **19**, 1251–1254.
- Ehara, S., Muramatsu, K., Shimazu, M., Tanaka, J., Tsukioka, M., Mori, Y. et al., Dielectric properties of Bi<sub>4</sub>Ti<sub>3</sub>O<sub>12</sub> below the Curie temperature. *Jpn. J. Appl. Phys.*, 1981, **20**, 877–881.
- Damjanovic, D., Ferroelectric, dielectric and piezoelectric properties of ferroelectric thin films and ceramics. *Rep. Prog. Phys.*, 1998, **61**, 1267–1324.
- Nakamura, T., Takashige, M., Terauchi, H., Miura, Y. and Lawless, W. N., The structural, dielectric, Raman-spectral and low-temperature properties of amorphous PbTiO<sub>3</sub>. *Jpn. J. Appl. Phys.*, 1984, **23**, 1265–1273.
- Qu, B. D., Jiang, B., Wang, Y. G., Zhang, P. L. and Zhong, W. L., Size and temperature-dependence of dielectric constant of ultrafine PbTiO<sub>3</sub> particles. *Chin. Phys. Lett.*, 1994, **11**, 514–517.
- Buessem, W. R., Cross, L. E. and Goswami, A. K., Phenomenological theory of high permittivity in fine-grained barium titanate. *J. Am. Ceram. Soc.*, 1966, **49**, 33–36.
- Arlt, G., Hennings, D. and With, G., Dielectric properties of fine-grained barium titanate ceramics. *J. Appl. Phys.*, 1985, **58**, 1619–1625.
- Su, D., Zhu, J. S., Xu, Q. Y., Liu, J. S. and Wang, Y. N., Transmission electron microscopy study on domain structures in Bi<sub>3</sub>TiNbO<sub>9</sub> ceramics. *Microelectron. Eng.*, 2003, **66**, 825–829.

27. Pribosic, I., Makovec, D. and Drogenik, M., Electrical properties of donor- and acceptor-doped  $\text{BaBi}_4\text{Ti}_4\text{O}_{15}$ . *J. Eur. Ceram. Soc.*, 2001, **21**, 1327–1331.
28. Huang, Y. N., Wang, Y. N. and Shen, H. M., Internal friction and dielectric loss related to domain walls. *Phys. Rev. B*, 1992, **46**, 3290–3295.
29. Shulman, H. S., Damjanovic, D. and Setter, N., Niobium doping and dielectric anomalies in bismuth titanate. *J. Am. Ceram. Soc.*, 2000, **83**, 528–532.
30. Kingery, W. D., Bowen, H. K. and Uhlmann, D. R., *Introduction to ceramics (2nd ed.)*. John Wiley & Sons Inc., New York, 1976, p. 923.
31. Wang, Z., Chen, T., Zhu, W., Fu, J., Yan, H. and Li, C., Low-frequency internal friction study for SBTO ferroelectric ceramics. *Acta Phys. Sin. OV ED*, 1998, **7**, 764–772.
32. Yan, F., Chen, X. B., Bao, P. and Wang, Y. N., Internal friction and Young's modulus of  $\text{SrBi}_2\text{Ta}_2\text{O}_9$  ceramics. *J. Appl. Phys.*, 2000, **87**, 1453–1457.
33. Zhang, Q. M., Pan, W. Y., Jang, S. J. and Cross, L. E., Domain wall excitations and their contributions to the weak-signal response of doped lead zirconate titanate ceramics. *J. Appl. Phys.*, 1988, **64**, 6445–6451.
34. Zhang, Q. M., Wang, H., Kim, N. and Cross, L. E., Direct evaluation of domain-wall and intrinsic contributions to the dielectric and piezoelectric response and their temperature dependence on lead zirconate-titanate ceramics. *J. Appl. Phys.*, 1994, **75**, 454–459.
35. Reaney, I. M. and Damjanovic, D., Crystal structure and domain-wall contributions to the piezoelectric properties of strontium bismuth titanate ceramics. *J. Appl. Phys.*, 1996, **80**, 4223–4225.
36. Damjanovic, D., Demartin, M., Shulman, H. S., Testorf, M. and Setter, N., Instabilities in the piezoelectric properties of ferroelectric ceramics. *Sens. Actuators A*, 1996, **53**, 353–360.
37. Sagalowicz, L., Chu, F., Martin, P. D. and Damjanovic, D., Microstructure, structural defects, and piezoelectric response of  $\text{Bi}_4\text{Ti}_3\text{O}_{12}$  modified by  $\text{Bi}_3\text{TiNbO}_9$ . *J. Appl. Phys.*, 2000, **88**, 7258–7263.
38. Hong, S. H., Trolier-Mckinstry, S. and Messing, G. L., Dielectric and electromechanical properties of textured niobium-doped bismuth titanate ceramics. *J. Am. Ceram. Soc.*, 2000, **83**, 113–118.